



The Impact of Image Reconstruction Parameters on TARE Treatment Dosimetric Calculation

Bilal Kovan^{1*} , Emine Gökür Işık¹ 

¹ Istanbul University, Istanbul Faculty of Medicine, Department of Nuclear Medicine, Istanbul, Türkiye

*bkovan@istanbul.edu.tr

* Orcid No: 0000-0002-4431-8358

Received: 4 May 2024

Accepted: 7 June 2024

DOI: 10.18466/cbayarfb.1478468

Abstract

Accurate dosimetric calculations are essential to enhance therapeutic efficacy in Yttrium-90 (Y-90) microsphere therapy, which rely significantly on the three-dimensional imaging parameters used. This study aims to evaluate the reconstruction parameters used to generate three-dimensional images from SPECT data obtained for dosimetric calculations, and to determine the optimal reconstruction parameters. This retrospective study evaluated Single Photon Emission Computed Tomography/Computed Tomography (SPECT/CT) images of 30 patients (8 women and 22 men) who underwent Transarterial Radioembolization (TARE) treatment at our clinic between 2018 and 2019 using Technetium 99mTc-labeled macroaggregated albumin (99mTc-MAA). The SPECT images were reconstructed using 20 different iterations and subset values. The perfused areas were identified using 5% and 10% threshold values. At the 5% threshold, the maximum difference from the average was 20.7% at 2 iterations and 2 subsets. For other parameters, the difference from the average was less than 2.8%. At the 10% threshold, the maximum difference from the average was 14.8% at 2 iterations and 2 subsets, with other parameters again showing a difference of less than 2.8%. For effective TARE treatment, it is recommended to set the SPECT image reconstruction parameters to higher than 5 iterations and 5 subsets following the administration of 99mTc-MAA.

Keywords: Dosimetry, Iteration, Subset, Radioembolization, SPECT

1. Introduction

Selective Internal Radiation Therapy (SIRT), also known as Yttrium-90 (Y-90) microsphere transarterial radioembolization (TARE), is an established and promising treatment modality for primary liver tumors and liver metastases [1, 2]. The objective of TARE treatment is to deliver the maximum radiation dose to the tumors while minimizing exposure to the healthy parenchymal tissue [3]. In TARE treatment, radioactive microspheres are injected into the tumor region through the arteries that feed the tumor [4]. A pre-treatment evaluation is conducted to determine the patient's suitability for the treatment. Due to 90Y being a pure beta emitter, the treatment evaluation utilizes Technetium 99mTc-labeled macroaggregated albumin (99mTc-MAA) which mimics the microspheres [4]. This evaluation is crucial for determining the risk of lung shunting, controlling gastric leakage, and, most importantly, for dose planning [5-7]. After the

administration of 99mTc-MAA, whole-body and Single Photon Emission Computed Tomography/Computed Tomography (SPECT/CT) imaging of the patient should be performed as soon as possible [8]. Using the obtained images, patient suitability is assessed and the dose to be administered is calculated. Scientific studies have shown that personalized dosimetry calculations significantly affect TARE treatment's effectiveness [1, 9]. In the international multicenter study conducted by Lam et al. and the European Association of Nuclear Medicine (EANM) treatment guideline, it was stated that dosimetric calculation should be made in TARE treatment and that dosimetry increases the effectiveness of treatment.

Despite not being fully standardized, dosimetric calculation protocols in Nuclear Medicine therapeutic applications are continually being refined through numerous scientific studies. Recently, international bodies have published dosimetry guidelines for nuclear medicine treatments [10-12]. All guidelines advocate

using the Medical Internal Radiation Dose (MIRD) formula for calculations [12, 13]. Data derived from patient imaging are used in the MIRD formula. For error-free dosimetry, imaging protocols and image formation parameters must be tailored to the specific application. The EANM guidelines offer recommendations for SPECT/CT and Positron Emission Tomography (PET)/CT imaging post-procedure and treatment [12]. These guidelines specify parameters that should be used during imaging: low-energy collimators, matrix sizes of 256×256 or 128×128 , an energy window centered at 140 keV with a 15% width for the main peak, adjacent scatter energy windows, 30-degree projection angles, and a minimum of 15 seconds per projection. Detailed information regarding the parameters necessary for three-dimensional image reconstruction is not provided. The EANM guidelines emphasize the need for optimization in voxel dosimetry, suggesting that the number of iterations and subsets typically used for diagnostic purposes should be higher.

The aim of this study is to determine how different iteration and subset values used in image reconstruction of TARE treatment evaluation images affect dosimetric calculations and to establish the optimal reconstruction parameters for TARE treatment evaluations.

2. Materials and Methods

2.1 Patients and Sample Collection

The collection of human samples for this study was approved by the Ethics Committee of the Istanbul Medical Faculty (Protocol number: 2024/918).

This retrospective study included 30 patients treated with ^{99m}Tc -MAA and underwent Hepatic Artery Perfusion Scintigraphy (HAPS) at our clinic during the years 2018-2019, consisting of 8 women and 22 men. The inclusion criteria were patients older than 18 years, suitable for TARE treatment without any contraindications in mapping scintigraphy.

2.2 Hepatic Artery Perfusion Scintigraphy Data Acquisition

An hour after administering 185-222 MBq/5 ml of ^{99m}Tc -labeled macro aggregated albumin (MAA) for simulation angiography ahead of Transarterial Radioembolization (TARE) treatment with Therasphere from BTG International Ltd., Ottawa, Canada, whole-body anterior and posterior planar imaging was conducted using a GE Discovery NM 670 SPECT/CT system (General Electric Healthcare, Waukesha, WI, USA). Equipped with a low-energy high-resolution (LEHR) collimator and a primary energy peak of 140.5 keV ($\pm 10\%$), the system utilized a window gap set to a 128×128 matrix, with imaging parameters established at 13 cm/min. Subsequently, SPECT imaging was performed on both lung and abdominal regions,

employing a primary energy peak of 140.5 keV ($\pm 10\%$) and a scatter peak of 120 keV ($\pm 5\%$), comprising 60 frames captured over 20 seconds each. Following SPECT imaging, a CT scan of the same regions ensued, facilitating anatomical correlation and attenuation correction, with settings at 120 keV and 100 mAs.

2.3 Image Reconstruction

The acquired SPECT and CT data were processed using the ordered-subset expectation maximization (OSEM) method, using the Butterworth filter and CT-based attenuation correction. Image processing has been reconstructed using iteration-subset values are respectively; 2-2 (C1), 2-5 (C2), 2-10 (C3), 2-20 (C4), 5-5 (C5), 5-10 (C6), 5-15 (C7), 5-20 (C8), 10-5 (C9), 10-10 (C10), 10-15 (C11), 10-20 (C12), 15-5 (C13), 15-10 (C14), 15-15 (C15), 15-20 (C16), 20-5 (C17), 20-10 (C18), 20-15 (C19) and 20-20 (C20).

2.4 Data Analysis

All image analyses were conducted using the Mirada DBx 1.2.0 and Simlicit90Y dosimetry software. The volume and count values of the perfused areas were determined using threshold values of 5% and 10%. The changes in these values according to different iteration and subset changes were analyzed.

2. Results and Discussion

The volumes of perfused areas at the 5% threshold were presented in Table 1, and at the 10% threshold in Table 2. The counts of perfused areas at the 5% threshold were presented in Table 3, and at the 10% threshold in Table 4. Considering these values, the average perfused area volumes at 5% threshold for the thirty patients according to configurations C1 through C20 were as follows: 1043.3, 884.1, 860.7, 844.6, 860.6, 856.5, 863.4, 846.6, 858.4, 851.9, 858.8, 841.9, 858.3, 850.1, 856.4, 840.3, 858.3, 852.7, 858.8, and 841.5 cm^3 , respectively. The greatest variance from the average was 20.7% observed in C1, while other configurations showed differences of less than 2.8%. The counts were as follows: 5,082,759, 5,658,949, 5,664,377, 5,595,932, 5,710,880, 5,680,083, 5,554,952, 5,597,601, 5,717,349, 5,683,208, 5,559,058, 5,601,691, 5,718,115, 5,682,599, 5,557,861, 5,599,595, 5,725,705, 5,686,537, 5,561,944, and 5,628,692. The highest variance from the average count was 9.5% in C1, with other configurations showing less than 2%.

For the 10% threshold, the perfused area volumes for C1 through C20 were as follows: 722, 648, 630, 615, 634, 624, 624, 609, 632, 626, 622, 611, 631, 623, 622, 611, 630, 623, 622, and 612 cm^3 , respectively. The greatest difference from the average was 14.8% for C1, with other configurations showing differences of less than 2.8%. The counts were as follows: 4,566,302, 5,050,578, 5,058,360, 4,991,871, 4,983,310, 5,037,283, 5,086,541,

4,989,636, 5,109,255, 5,077,754, 4,937,672, 4,991,870, 5,109,296, 5,078,857, 5,071,626, 4,994,661, 5,114,986, 5,077,171, 5,057,384, and 4,991,746. The highest difference from the average count was 9% in C1, with other configurations showing differences of less than 1.9%.

Regarding the distribution of perfused area sizes for the 10% threshold: 12 patients had areas under 500 cm³, 11 patients between 500 cm³ and 1000 cm³, and 7 patients had areas over 1000 cm³. The greatest difference from the average volume for areas under 500 cm³ was 4.7% at C8 for the 10% threshold, with other configurations showing differences of less than 4.6%. At the 5% threshold, the greatest difference was 10.7% in C1, with other configurations showing differences of less than 3.8%. Count variances were 9.2% at the 5% threshold and 10.2% at the 10% threshold for C1.

For patients with perfused areas between 500 and 1000 cm³, the greatest difference from the average volume was 11.5% at C1 for the 10% threshold, with other configurations showing differences of less than 3.6%. At the 5% threshold, the greatest difference was 17.8% at C1, with other configurations showing differences of less than 3.7%. Count variances were 10.4% at the 5% threshold and 18.2% at the 10% threshold for C1.

For patients with perfused areas over 1000 cm³, the greatest difference from the average volume was 18.9% at C1 for the 10% threshold, with other configurations showing differences of less than 4%. At the 5% threshold, the greatest difference was 25.3% at C1, with other configurations showing differences of less than 3.1%. Count variances were 8.4% at the 5% threshold and 8.9% at the 10% threshold for C1.

Recent years have seen an acceleration in research focusing on the importance of dosimetry and its contribution to the efficacy of TARE treatment. The acquisition parameters for SPECT imaging and reconstruction, particularly for voxel-based dosimetry, are crucial. International authorities emphasize the need for well-defined imaging acquisition and reconstruction parameters, which directly affect treatment effectiveness.

In this study, following the administration of 99mTc-MAA for TARE treatment, the impact of image reconstruction parameters on perfused areas and counts was investigated. Variations were observed with different iteration and subset values. The highest deviation from the average in perfused areas was found in images with 2 iterations and 2 subsets at both 5% and 10% threshold values, where the perfused area values were calculated to be 20.7% and 14.8% higher than average, respectively. This suggests a potential increase of up to 20.7% in the treatment dose applied to patients. For images with 2 iterations and 5 subsets, the increase was 2.3% at a 5% threshold and 3.1% at a 10% threshold. Other iteration and subset values calculated perfused areas closely together. It was found that while the number

of iterations did not change the perfused area, increasing the subset value tended to decrease the perfused area by approximately 3%.

When examining changes between iteration and subset values in counts, a 9.5% and 9% decrease from the average was detected in images with 2 iterations and 2 subsets at 5% and 10% thresholds, respectively. The counts in other values were closely aligned. These results indicate that settings below 5 iterations and 5 subsets tend to provide a high perfused area with a low count.

The relationship between the size of the perfused area and the changes in the perfused area and count ratios was also examined. Among the patients, 12 had a perfused area smaller than 500 cm³ (Group 1), 11 had between 500 cm³ and 1000 cm³ (Group 2), and 7 had more than 1000 cm³ (Group 3). The findings indicate minor deviations in Group 1, while deviations increased in Groups 2 and 3, particularly in configurations C1 and C2, correlating the size of the perfused area with the deviation observed.

No similar studies exist for imaging post 99mTc-MAA application in TARE treatment. However, several studies are available on imaging acquisition parameters and image reconstruction for scattering and attenuation correction. Research evaluating iteration and subset values in post-treatment imaging with 90Y has been conducted [14, 15]. A study by Linder et al. explored post-treatment PET imaging parameters with 90Y, reporting the best results with 2 iterations and 5 subsets, a 4 mm filter, and a 20-minute scanning time [14]. Considering 90Y's pure beta emission and the imaging being conducted with bremsstrahlung radiation, our study results differ. Costa and colleagues also performed phantom and patient imaging with 90Y using two different PET machines [15], utilizing OSEM, 4 iterations, and 20 subsets, which were deemed suitable for dosimetry.

In a phantom study by Cheenu Kappadath, diagnostic imaging reconstruction parameters with 99mTc were evaluated. Images obtained with different iteration and subset values were compared, finding that high-background images performed best with 20 iterations and 18 subsets, while no-background images were optimal with 10 iterations and 18 subsets [16]. He also emphasized that the specificity of iterative reconstruction parameters (iterations, subsets, and filtering) affects the quantitative outcome in SPECT, dependent on the nature of activity distribution within the SPECT field of view. His study, parallel to ours, recommended high iteration and subset values.

Our study shows that low iteration and subset values increase perfused area while decreasing counts, dependent on the size of the perfused area. It was determined that volume and count values do not change when iteration and subset values are above 5.

Recent studies emphasize the benefits of voxel-based dosimetric calculation for TARE treatments [17-19]. In voxel-based dosimetry, calculations are made based on activity distribution. Activity distribution is determined by the counts in SPECT images. In the study conducted by Coskun et al., treatment response was evaluated with voxel-based dosimetry and dose-volume histograms, and they emphasized that treatment response could be predicted with voxel-based dosimetry [20]. This shows that count and distribution are important in SPECT data in voxel-based dosimetry. It was observed that the counting rates decreased especially in low iteration and low subset values, and this rate increased especially in large volumes. It was observed that background decreased as the iteration and subset value increased. These results show that iteration and subset values will affect voxel-based dosimetry.

3. Conclusion

In the conclusion, the effect of reconstruction on dosimetry calculations is significant. We recommend setting SPECT image reconstruction parameters higher than 5 iterations and 5 subsets following the administration of ^{99m}Tc -MAA for TARE treatment.

Author's Contributions

Bilal Kovan: Drafted and wrote the manuscript, performed the experiment and result analysis.

Emine Gökknur Işık: Performed the experiment and result analysis.

Acknowledgement

There are no financial declarations. This work is not grant funded.

Ethics

The collection of human samples for this study was approved by the Ethics Committee of the Istanbul Medical Faculty (Protocol number: 2024/918).

References

[1]. Lam M, Garin E, et al. A global evaluation of advanced dosimetry in transarterial radioembolization of hepatocellular carcinoma with Yttrium-90: the TARGET study. *European Journal of Nuclear Medicine and Molecular Imaging*. 2022;49:3340-52.

[2]. Ramdhani K, Braat A. The Evolving Role of Radioembolization in the Treatment of Neuroendocrine Liver Metastases. *Cancers*. 2022;14.

[3]. Mikell JK, Dewaraja YK, et al. Transarterial Radioembolization for Hepatocellular Carcinoma and Hepatic Metastases: Clinical Aspects and Dosimetry Models. *Seminars in radiation oncology*. 2020;30:68-76.

[4]. Weber M, Lam M, et al. EANM procedure guideline for the treatment of liver cancer and liver metastases with intra-arterial

radioactive compounds. *European Journal of Nuclear Medicine and Molecular Imaging*. 2022;49:1682-99.

[5] Kovan B, Civan C, et al. Influencing factors of lung shunt fraction in transarterial radioembolization treatment. *Clinical and Translational Imaging*. 2024, 12.2: 205-211.

[6] Yilmaz E, Engin MN, et al. Y90 selective internal radiation therapy and peptide receptor radionuclide therapy for the treatment of metastatic neuroendocrine tumors: combination or not? *Nuclear Medicine Communications*. 2020;41:1242-9.

[7] Abuqbeith M, Demir M. Effect of predicted lung mass versus fixed mass regimes on lung dose in SIRT (90Y). *International Journal of Computational and Experimental Science and Engineering*. 2024;10.

[8] Kovan B, Denizmen D, et al. Influence of Early Versus Delayed Hepatic Artery Perfusion Scan on (90Y) Selective Internal Radiation Therapy Planning. *Cancer Biotherapy and Radiopharmaceuticals*. 2024.

[9] Guiu B, Garin E, et al. TARE in Hepatocellular Carcinoma: From the Right to the Left of BCLC. *Cardiovascular Interventional Radiology*. 2022;45:1599-607.

[10] Busse NC, Al-Ghazi MS, et al. AAPM Medical Physics Practice Guideline 14. a: Yttrium-90 microsphere radioembolization. *Journal of Applied Clinical Medical Physics*. 2024;25:e14157.

[11] Dezar WA, Cessna JT, et al. Recommendations of the American Association of Physicists in Medicine on dosimetry, imaging, and quality assurance procedures for 90Y microsphere brachytherapy in the treatment of hepatic malignancies. *Medical Physics*. 2011;38:4824-45.

[12] Chiesa C, Sjogreen-Gleisner K, et al. EANM dosimetry committee series on standard operational procedures: a unified methodology for (99m)Tc-MAA pre- and (90Y) peri-therapy dosimetry in liver radioembolization with (90Y) microspheres. *EJNMMI Physics*. 2021;8:77.

[13] Marquis H, Ocampo Ramos JC, et al. MIRDo90-A (90Y) Research Microsphere Dosimetry Tool. *Journal of Nuclear Medicine*. 2024.

[14] Linder PM, Lan W, et al. Optimization of Y-90 Radioembolization Imaging for Post-Treatment Dosimetry on a Long Axial Field-of-View PET/CT Scanner. *Diagnostics*. 2023;13.

[15] Costa G, Spencer B, et al. Radioembolization Dosimetry with Total-Body (90Y) PET. *Journal of Nuclear Medicine*. 2022;63:1101-7.

[16] Kappadath SC. Effects of voxel size and iterative reconstruction parameters on the spatial resolution of ^{99m}Tc SPECT/CT. *Journal of Applied Clinical Medical Physics*. 2011;12:3459.

[17] Orcajo Rincón J, Regi AR, et al., "Maximum tumor-absorbed dose measured by voxel-based multicompartmental dosimetry as a response predictor in yttrium-90 radiation segmentectomy for hepatocellular carcinoma," (in eng), *EJNMMI Physics*, vol. 10, no. 1, p. 7, Feb 6 2023, doi: 10.1186/s40658-022-00520-9.

[18] Villalobos A, Arndt L, et al., "Yttrium-90 Radiation Segmentectomy of Hepatocellular Carcinoma: A Comparative Study of the Effectiveness, Safety, and Dosimetry of Glass-Based versus Resin-Based Microspheres," (in eng), *Journal of Vascular and Interventional Radiology*, vol. 34, no. 7, pp. 1226-1234, Jul 2023, doi: 10.1016/j.jvir.2023.02.030.

[19] Yoo M. Y., Paeng JC, et al., "Efficacy of voxel-based dosimetry map for predicting response to trans-arterial radioembolization therapy for hepatocellular carcinoma: a pilot study," (in eng), *Nuclear Medicine Communications*, vol. 42, no. 12, pp. 1396-1403, Dec 1 2021, doi: 10.1097/mnm.0000000000001471.



[20] Coskun N, Kartal MO, et al., "Use of dose-volume histograms for metabolic response prediction in hepatocellular carcinoma patients undergoing transarterial radioembolization with Y-90 resin microspheres," (in eng), *Annals of Nuclear Medicine*, Apr 22 2024, doi: 10.1007/s12149-024-01926-4.



Appendix

Table 1. Volumes (cm³) with 5% threshold in all configurations.

Patient No	C1	C2	C3	C4	C5	C6	C7	C8	C9	C10	C11	C12	C13	C14	C15	C16	C17	C18	C19	C20
1	357	315	312	335	312	312	301	314	306	325	303	324	309	315	303	324	311	312	316	315
2	213	205	209	200	207	210	214	200	207	211	214	200	207	211	214	200	207	211	214	200
3	234	209	221	195	206	221	206	195	206	222	206	196	207	223	206	196	207	223	206	195
4	137	120	117	117	120	117	119	117	120	117	119	117	120	116	119	117	120	117	119	117
5	97	89	101	91	90	91	90	101	91	91	90	101	90	91	90	98	90	91	90	97
6	194	162	160	158	159	160	158	158	159	160	159	159	159	160	158	159	159	160	159	159
7	334	301	279	247	311	283	323	244	314	285	326	244	315	287	326	244	316	287	326	244
8	270	225	214	217	219	214	216	217	218	214	216	217	219	215	217	216	219	215	217	216
9	68	63	61	57	64	61	61	57	65	62	61	57	64	62	61	57	64	62	61	57
10	471	463	455	454	479	459	493	453	480	460	494	454	480	460	494	455	480	461	493	456
11	441	398	395	387	398	397	398	388	399	397	398	388	400	396	400	387	400	397	400	387
12	227	207	204	201	205	204	201	202	205	205	202	202	205	205	202	202	206	205	202	202
13	1115	943	894	834	876	867	993	833	860	867	998	833	859	870	996	833	860	870	996	822
14	951	847	807	760	816	806	828	764	816	807	804	761	817	807	804	764	796	808	803	763
15	815	695	689	660	682	691	695	645	678	688	694	662	685	691	698	663	688	697	699	664
16	977	862	847	845	842	844	837	850	839	844	837	851	839	845	837	850	840	846	835	851
17	763	667	658	678	559	662	667	676	663	662	667	673	671	661	667	674	672	660	667	674
18	1147	943	893	834	876	867	993	833	860	867	998	833	859	870	996	833	860	870	996	833
19	1285	1114	1083	1065	1081	1062	1065	1056	1069	1061	1061	1056	1066	1061	1061	1056	1067	1058	1061	1056
20	1154	1022	1014	1009	1021	1016	1034	1008	1022	1015	1035	1008	1022	1015	1034	1008	1024	1016	1035	1003
21	1095	941	906	883	930	901	880	881	932	902	881	877	933	901	881	878	934	897	882	878
22	2072	1727	1680	1683	1684	1667	1668	1678	1674	1667	1668	1678	1672	1664	1666	1678	1670	1664	1665	1681
23	2458	1952	1861	1879	1897	1862	1866	1873	1893	1861	1850	1856	1874	1860	1834	1856	1874	1844	1833	1855
24	1834	1565	1484	1516	1521	1482	1441	1515	1517	1483	1446	1514	1516	1483	1446	1514	1516	1483	1446	1518
25	1859	1575	1546	1537	1536	1539	1547	1533	1534	1541	1548	1536	1536	1540	1547	1532	1536	1541	1543	1533
26	1411	1268	1230	1214	1245	1220	1210	1211	1234	1217	1214	1210	1232	1217	1214	1204	1232	1218	1214	1203
27	2952	2503	2428	2388	2410	2382	2349	2354	2404	2381	2310	2362	2404	2382	2310	2353	2404	2383	2313	2377
28	2949	2168	2056	2040	2075	2049	2041	2019	2085	2049	2046	2016	2088	2054	2041	2015	2088	2059	2045	2016
29	1387	1229	1214	1114	1217	1211	1207	1201	1213	1210	1206	1201	1205	1209	1206	1162	1204	1210	1207	1193
30	2032	1747	1804	1742	1783	1839	1800	1822	1689	1686	1716	1673	1695	1634	1665	1684	1707	1720	1723	1683
Mean	1043	884	861	845	861	857	863	847	858	852	859	842	858	850	856	840	858	853	859	842

C: Configuration



Table 2. Volumes (cm³) with 10% threshold in all configurations.

Patient No	C1	C2	C3	C4	C5	C6	C7	C8	C9	C10	C11	C12	C13	C14	C15	C16	C17	C18	C19	C20
1	237	217	215	218	215	215	200	211	214	212	202	215	214	222	202	227	216	214	210	227
2	121	118	124	116	121	126	129	116	122	127	130	117	123	127	130	116	123	127	130	116
3	159	150	164	146	152	164	152	147	153	164	152	147	153	165	152	147	152	165	152	147
4	96	89	87	88	90	87	88	88	90	87	88	88	90	87	88	88	90	88	88	88
5	63	61	70	64	63	64	63	71	63	64	63	71	63	64	64	69	63	64	64	68
6	134	120	120	120	120	121	118	120	120	121	119	120	120	121	119	120	120	121	119	120
7	164	143	135	111	143	136	154	111	144	136	155	111	145	137	155	111	145	137	155	111
8	183	170	166	170	169	166	164	169	166	166	163	169	168	166	163	169	168	166	163	169
9	45	44	43	41	44	43	43	41	44	43	43	41	44	43	43	41	44	43	43	40
10	188	187	189	192	196	192	209	194	199	193	210	194	199	193	210	193	199	193	210	193
11	264	251	250	241	250	251	252	242	252	252	252	241	252	251	253	241	253	251	252	241
12	149	142	141	141	143	142	140	142	144	143	141	142	144	143	141	142	144	143	141	142
13	720	624	593	537	579	572	647	531	566	570	648	533	564	571	647	533	564	570	647	533
14	606	557	529	478	545	519	540	476	531	519	528	474	531	519	527	475	520	520	528	475
15	570	529	530	512	526	528	532	508	525	530	533	513	525	530	534	514	525	531	535	514
16	664	604	599	594	592	599	599	600	592	598	598	600	593	599	599	600	593	599	598	601
17	543	504	499	514	510	499	506	511	509	498	507	511	510	497	508	511	510	497	508	511
18	720	624	593	538	579	572	647	532	566	570	648	533	564	571	647	533	564	570	647	533
19	942	892	890	883	889	884	880	878	885	883	878	875	883	883	878	875	883	882	878	875
20	804	758	754	747	764	757	775	745	765	757	777	744	765	758	776	744	766	758	776	744
21	706	627	593	571	625	591	574	568	627	592	575	566	626	593	572	563	627	589	572	563
22	1546	1339	1302	1307	1303	1285	1284	1300	1292	1278	1278	1297	1286	1274	1275	1296	1282	1272	1274	1297
23	1741	1426	1367	1388	1394	1366	1362	1383	1387	1367	1347	1375	1379	1359	1341	1368	1371	1351	1340	1368
24	1360	1223	1149	1188	1205	1151	1111	1092	1206	1153	1114	1191	1207	1153	1113	1190	1208	1156	1115	1192
25	1408	1296	1295	1279	1278	1290	1289	1277	1280	1289	1289	1274	1274	1288	1287	1272	1279	1288	1284	1272
26	939	884	850	842	860	841	833	837	856	840	836	837	857	840	839	833	858	840	839	833
27	2063	1947	1864	1738	1883	1833	1733	1705	1878	1828	1710	1705	1874	1806	1710	1705	1847	1805	1710	1711
28	2040	1643	1539	1497	1564	1515	1487	1481	1553	1514	1484	1482	1552	1512	1483	1481	1551	1511	1483	1481
29	1034	997	990	920	990	982	973	956	986	981	966	955	979	982	966	935	978	981	966	948
30	1448	1271	1247	1263	1232	1241	1246	1242	1229	1291	1241	1221	1251	1247	1245	1239	1250	1266	1250	1240
Mean	722	648	630	615	634	624	624	609	632	626	622	611	631	623	622	611	630	623	622	612

C: Configuration



Table 3. Counts with 5% threshold in all configurations.

Patient No	C1	C2	C3	C4	C5	C6	C7	C8	C9	C10	C11	C12	C13	C14	C15	C16	C17	C18	C19	C20
1	5709444	6213757	6245399	6202018	6258549	6262030	6195192	6183866	6245058	6319060	6203690	6221820	6257946	6278391	6205659	6221199	6270220	6266000	6259788	6187308
2	5933652	6683319	6735070	6940234	6809696	6771455	6707650	6942021	6829010	6779550	6708804	6940794	6830380	6783747	6712714	6943597	6832780	6784342	6712336	6942793
3	2623428	2882474	2865983	2776991	2908121	2875822	2842757	2778683	2912408	2880247	2843441	2780865	2916348	2881733	2842684	2780472	2917272	2881915	2842951	2780251
4	4118512	4477931	4441838	4580624	4508699	4448080	4450214	4585026	4514132	4450482	4450211	4583933	4514016	4449236	4449865	4585346	4514156	4451159	4449669	4584852
5	647087	708895	749869	720056	718065	722125	727919	755556	719148	722754	727957	757643	719166	722854	728432	743024	719479	722546	728137	734318
6	3815546	4134746	4154899	4076060	4158883	4162025	4129047	4079225	4164056	4164813	4130980	4081123	4164849	4164367	4130415	4080040	4166278	4164212	4130965	4081123
7	4426761	4383675	4451215	3230242	4486877	4495272	5885056	3220899	4515732	4511654	5900376	3221426	4526896	4518505	5901526	3220571	4530548	4522090	5903815	3220147
8	1862074	2021630	2054923	1978425	2039369	2061243	2045323	1983252	2043242	2063782	2045720	1980246	2046012	2064265	2045917	1979123	2046852	2064565	2046608	1979025
9	4454448	4828652	4869154	4706963	4872536	4875677	4844999	4714409	4878319	4882331	4843052	4709585	4877915	4882654	4842915	4709789	4878546	4881344	4844228	4709852
10	8174582	9417541	9539452	9523654	9695241	9623541	9785214	9524569	9736214	9635547	9790854	9535625	9747852	9645879	9791325	9547852	9753652	9658541	9788745	9549236
11	5582897	6093425	6161556	5996461	6150416	6192635	6114798	6006785	6174325	6199854	6117854	6008125	6180254	6198745	6123654	6007145	6182456	6200652	6123562	6007545
12	5586398	6264999	6330842	6173155	6321359	6349521	6186025	6182563	6335680	6356048	6198547	6188063	6345896	6359052	6198874	6188095	6345214	6362541	6198797	6183652
13	9616032	10354736	9995623	10124578	10317854	9955602	7414215	10129654	10300306	9966325	7429778	10139547	10302547	9977458	7425412	10132547	10311145	9987632	7425645	10132546
14	670765	731125	737261	750754	734535	740025	747458	751421	736852	741021	742565	750325	737785	741956	742789	750896	733632	741445	742635	750752
15	6988130	7678099	7732654	7666965	7759856	7765645	7809152	7608090	7764125	7767075	7809654	7678109	7785748	7776625	7822415	7681034	7795748	7792013	7823698	7682785
16	4622356	4990125	5043215	4975825	5036251	5063215	5094754	4985632	5042154	5069125	5096325	4985632	5047545	5071021	5096452	4985625	5050565	5073652	5093256	4988965
17	4587676	4931093	4975785	5119232	4985214	4993939	5096541	5112962	4978965	4999965	5098365	5178960	4998965	4997854	5098854	5110454	5001545	4997898	5099797	5110452
18	9616017	10354736	9995623	10122441	10318702	9955602	7414277	10129773	10300306	9966601	7429778	10132382	10305969	9977760	7427381	10123203	10311452	9978637	7427457	10134579
19	5468974	5998874	6059673	6037584	6078654	6082854	6090025	6040452	6095745	6090845	6089254	6041452	6100125	6095841	6090145	6041578	6103025	6091542	6090033	6041525
20	10704512	11578965	11529564	11535326	11690631	11563728	11784855	11540854	11716854	11567654	11790021	11544475	11721546	11570354	11790054	11545302	11726988	11572525	11795846	11527799
21	30579	3341563	3261953	3348558	3362356	3268565	3145326	3351125	3372965	3273562	3146025	3348256	3373652	3274125	3146852	3349521	3378011	3269984	3147589	3349587
22	9511521	10481545	10568400	10528652	10573785	10585562	10560745	10528652	10585005	10591825	10563541	10530325	10588452	10588452	10560214	10530452	10586154	10589265	10560000	10537045
23	4163325	4512454	4521546	4512541	4533214	4539505	4500001	4519563	4543326	4544854	4494541	4512415	4538365	4545581	4486855	4512536	4540273	4538254	4486594	5413125
24	8348156	9146003	9107854	8600854	9200214	9138546	9367854	8615241	9220632	9145874	9378546	8611523	9226262	9148985	9379845	8611785	9227854	9151062	9385214	8618054
25	8302541	9065021	9095263	9002787	9128654	9117325	9203965	9009785	9146254	9125478	9208254	9016521	9016521	9126654	9208254	9013025	9156235	9128365	9204025	9015412
26	4454896	4947111	5005321	4958712	4986014	5013425	4848652	4958852	4988443	5015412	4954969	4949062	4990095	5015965	4954955	4958741	4991517	5017452	4955214	4953652
27	2049107	2305789	2335589	2402456	2321758	2339451	2313254	2388974	2331546	2345698	2305124	2392582	2334215	2344864	2305689	2390152	2335621	2345698	2306954	2403214
28	3241658	3442651	3449365	3426325	3456932	3464356	3432565	3421958	3475896	3468475	3436521	3421935	3481722	3471978	3433220	3425621	3483465	3475231	3435421	3422451
29	20867	23210	23107	22527	23521	23177	22526	23522	23569	23187	22528	23525	23544	23184	22530	23195	23546	23191	22533	23493
30	7150819	7774335	7893315	7836973	7890438	7952548	7888201	7854652	7830190	7827149	7814459	7784454	7842847	7779879	7769922	7795933	7856926	7862343	7826793	7795218
Mean	5082759	5658949	5664377	5595932	5710880	5680083	5554952	5597601	5717349	5683208	5559058	5601691	5718115	5682599	5557861	5599595	5725705	5686537	5561944	5628692

C: Configuration



Table 4. Counts with 10% threshold in all configurations.

Patient No	C1	C2	C3	C4	C5	C6	C7	C8	C9	C10	C11	C12	C13	C14	C15	C16	C17	C18	C19	C20
1	5709444	6213757	6245399	6202018	6258549	6262030	6195192	6183866	6245058	6319060	6203690	6221820	6257946	6278391	6205659	6221199	6270220	6266000	6259788	6187308
2	5933652	6683319	6735070	6940234	6809696	6771455	6707650	6942021	6829010	6779550	6708804	6940794	6830380	6783747	6712714	6943597	6832780	6784342	6712336	6942793
3	2623428	2882474	2865983	2776991	2908121	2875822	2842757	2778683	2912408	2880247	2843441	2780865	2916348	2881733	2842684	2780472	2917272	2881915	2842951	2780251
4	4118512	4477931	4441838	4580624	4508699	4448080	4450214	4585026	4514132	4450482	4450211	4583933	4514016	4449236	4449865	4585346	4514156	4451159	4449669	4584852
5	647087	708895	749869	720056	718065	722125	727919	755556	719148	722754	727957	757643	719166	722854	728432	743024	719479	722546	728137	734318
6	3815546	4134746	4154899	4076060	4158883	4162025	4129047	4079225	4164056	4164813	4130980	4081123	4164849	4164367	4130415	4080040	4166278	4164212	4130965	4081123
7	4426761	4383675	4451215	3230242	4486877	4495272	5885056	3220899	4515732	4511654	5900376	3221426	4526896	4518505	5901526	3220571	4530548	4522090	5903815	3220147
8	1862074	2021630	2054923	1978425	2039369	2061243	2045323	1983252	2043242	2063782	2045720	1980246	2046012	2064265	2045917	1979123	2046852	2064565	2046608	1979025
9	4454448	4828652	4869154	4706963	4872536	4875677	4844999	4714409	4878319	4882331	4843052	4709585	4877915	4882654	4842915	4709789	4878546	4881344	4844228	4709852
10	8174582	9417541	9539452	9523654	9695241	9623541	9785214	9524569	9736214	9635547	9790854	9535625	9747852	9645879	9791325	9547852	9753652	9658541	9788745	9549236
11	5582897	6093425	6161556	5996461	6150416	6192635	6114798	6006785	6174325	6199854	6117854	6008125	6180254	6198745	6123654	6007145	6182456	6200652	6123562	6007545
12	5586398	6264999	6330842	6173155	6321359	6349521	6186025	6182563	6335680	6356048	6198547	6188063	6345896	6359052	6198874	6188095	6345214	6362541	6198797	6183652
13	9616032	10354736	9995623	10124578	10317854	9955602	7414215	10129654	10300306	9966325	7429778	10139547	10302547	9977458	7425412	10132547	10311145	9987632	7425645	10132546
14	670765	731125	737261	750754	734535	740025	747458	751421	736852	741021	742565	750325	737785	741956	742789	750896	733632	741445	742635	750752
15	6988130	7678099	7732654	7666965	7759856	7765645	7809152	7608090	7764125	7767075	7809654	7678109	7785748	7776625	7822415	7681034	7795748	7792013	7823698	7682785
16	4622356	4990125	5043215	4975825	5036251	5063215	5094754	4985632	5042154	5069125	5096325	4985632	5047545	5071021	5096452	4985625	5050565	5073652	5093256	4988965
17	4587676	4931093	4975785	5119232	4985214	4993939	5096541	5112962	4978965	4999965	5098365	5178960	4998965	4997854	5098854	5110454	5001545	4997898	5099797	5110452
18	9616017	10354736	9995623	10122441	10318702	9955602	7414277	10129773	10300306	9966601	7429778	10132382	10305969	9977760	7427381	10123203	10311452	9978637	7427457	10134579
19	5468974	5998874	6059673	6037584	6078654	6082854	6090025	6040452	6095745	6090845	6089254	6041452	6100125	6095841	6090145	6041578	6103025	6091542	6090033	6041525
20	10704512	11578965	11529564	11535326	11690631	11563728	11784855	11540854	11716854	11567654	11790021	11544475	11721546	11570354	11790054	11545302	11726988	11572525	11795846	11527799
21	30579	3341563	3261953	3348558	3362356	3268565	3145326	3351125	3372965	3273562	3146025	3348256	3373652	3274125	3146852	3349521	3378011	3269984	3147589	3349587
22	9511521	10481545	10568400	10528652	10573785	10585562	10560745	10528652	10585005	10591825	10563541	10530325	10588452	10588452	10560214	10530452	10586154	10589265	10560000	10537045
23	4163325	4512454	4521546	4512541	4533214	4539505	4500001	4519563	4543326	4544854	4494541	4512415	4538365	4545581	4486855	4512536	4540273	4538254	4486594	5413125
24	8348156	9146003	9107854	8600854	9200214	9138546	9367854	8615241	9220632	9145874	9378546	8611523	9226262	9148985	9379845	8611785	9227854	9151062	9385214	8618054
25	8302541	9065021	9095263	9002787	9128654	9117325	9203965	9009785	9146254	9125478	9208254	9016521	9016521	9126654	9208254	9013025	9156235	9128365	9204025	9015412
26	4454896	4947111	5005321	4958712	4986014	5013425	4848652	4958852	4988443	5015412	4954969	4949062	4990095	5015965	4954955	4958741	4991517	5017452	4955214	4953652
27	2049107	2305789	2335589	2402456	2321758	2339451	2313254	2388974	2331546	2345698	2305124	2392582	2334215	2344864	2305689	2390152	2335621	2345698	2306954	2403214
28	3241658	3442651	3449365	3426325	3456932	3464356	3432565	3421958	3475896	3468475	3436521	3421935	3481722	3471978	3433220	3425621	3483465	3475231	3435421	3422451
29	20867	23210	23107	22527	23521	23177	22526	23522	23569	23187	22528	23525	23544	23184	22530	23195	23546	23191	22533	23493
30	7150819	7774335	7893315	7836973	7890438	7952548	7888201	7854652	7830190	7827149	7814459	7784454	7842847	7779879	7769922	7795933	7856926	7862343	7826793	7795218
Mean	5082759	5658949	5664377	5595932	5710880	5680083	5554952	5597601	5717349	5683208	5559058	5601691	5718115	5682599	5557861	5599595	5725705	5686537	5561944	5628692

C: Configuration